Translational Oncology
www.transonc.com

Volume 4 Number 5 October 2011 pp. 314–320 314

Immunohistochemical Staining of Slit2 in Primary and Metastatic Prostatic Adenocarcinoma[1]

Tanner L. Bartholow*, Michael J. Becich†, Uma R. Chandran† and Anil V. Parwani‡

*University of Pittsburgh School of Medicine, Pittsburgh, PA, USA; †Department of Biomedical Informatics, University of Pittsburgh School of Medicine, Pittsburgh, PA, USA; ‡Department of Pathology, University of Pittsburgh School of Medicine, Pittsburgh, PA, USA

Abstract

BACKGROUND: Conflicting roles for Slit2, a protein involved in mediating the processes of cell migration and chemotactic response, have been previously described in prostate cancer. Here we use immunohistochemistry to evaluate the expression of Slit2 in normal donor prostate (NDP), benign prostatic hyperplasia (BPH), high-grade prostatic intraepithelial neoplasia (HGPIN), normal tissue adjacent to prostatic adenocarcinoma (NAC), primary prostatic adenocarcinoma (PCa), and metastatic prostatic adenocarcinoma (Mets). *METHODS:* Tissue microarrays were immunostained for Slit2. The staining intensities were quantified using automated image analysis software. The data was statistically analyzed using one-way analysis of variance with subsequent Tukey tests for multiple comparisons or a nonparametric equivalent. Eleven cases of NDP, 35 cases of NAC, 15 cases of BPH, 35 cases of HGPIN, 106 cases of PCa, and 37 cases of Mets were analyzed. *RESULTS:* Specimens of PCa and HGPIN had the highest absolute staining for Slit2. Significant differences were seen between PCa and NDP ($P < .05$), PCa and NAC ($P < .05$), HGPIN and NDP ($P < .05$), and HGPIN and NAC ($P < .05$). Whereas the average Mets staining was not significantly different from NDP or NAC, several individual Mets cases featured intense staining. *CONCLUSIONS:* To our knowledge, this represents the first study comparing the immunohistochemical profiles of Slit2 in PCa and Mets to specimens of HGPIN, BPH, NDP, and NAC. These findings suggest that Slit2 expression can be increased in HGPIN, PCa, and Mets, making it a potentially important biomarker for prostate cancer.

Translational Oncology (2011) 4, 314–320

Introduction

Aside from basal and squamous cell carcinomas of the skin, prostate cancer is the most frequently occurring cancer in males, with more than 217,000 new cases estimated to have occurred in the United States during 2010. In addition, it is the second leading cause of male cancer mortality, responsible for an estimated 32,050 cancer deaths per year [1]. Despite this, after the implementation of prostate-specific antigen screening, researchers have estimated that clinically insignificant prostate cancer is actually overdiagnosed at a rate of 29% for whites and 44% for blacks [2]. Consequently, many researchers and clinicians have voiced a need for ways to discern high-risk patients in need of aggressive treatment from those in whom the consequences of overtreatment would outweigh the benefits [3,4].

Address all correspondence to: Tanner L. Bartholow, BS, Department of Pathology, UPMC - Shadyside Hospital, 5230 Centre Ave, Pittsburgh, PA 15232.
E-mail: bartholow.tanner@medstudent.pitt.edu

[1]This work was supported by the Clinical and Translational Science Institute Multidisciplinary Predoctoral Fellowship program, awarded through the Clinical and Translational Science Institute and the Institute for Clinical Research Educational Education at the University of Pittsburgh (grant nos. 5TL1RR024155-02 and 5TL1RR024155-05) to Tanner L. Bartholow. Additional funds were provided by the Doris Duke Charitable Foundation and by the Departments of Pathology and Biomedical Informatics at the University of Pittsburgh. The authors declare that they have no competing interests.
Received 21 April 2011; Revised 3 June 2011; Accepted 6 June 2011

1944-7124/11/ DOI 10.1593/tlo.11151

There is currently a limited amount of information in the literature on biomarkers with the potential to discern the clinical behaviors of prostate tumors [5]. Evaluating the expression of novel prostate cancer biomarkers may yield not only candidates for improved diagnosis but also prognosis prediction and therapy selection.

Slit2 is a secretory glycoprotein that maps to the gene locus 4p15.2 [6]. A homolog of the *Drosophila* protein Slit2, it exists with two other mammalian slit proteins, Slit1 and Slit3, all of which are characterized by four leucine-rich repeat domains at its N-terminus, a series of epidermal growth factor–like domains, a laminin G domain, and a cysteine-rich C-terminus [7]. As a ligand in the Slit/Robo system, Slit2 is responsible for guiding neural cell migration, where it has been demonstrated to prevent inappropriate midline axonal crossing events [8,9].

Functions for Slit2 outside the central nervous system have also been discovered. Among these functions are inhibiting leukocyte chemotaxis and vascular smooth muscle migration [10,11]. Interestingly, another work has also demonstrated that Slit2 is capable of attracting breast cancer cells [12].

The discovery of Slit2 as a guidance cue across multiple tissue types has prompted many studies to examine its potential as a biomarker for cancer, with two contrasting roles for Slit2 having been proposed, with some suggesting that it functions as a tumor suppressor, whereas others propose that it plays a role in oncogenesis.

Supporting the notion that Slit2 confers antitumorigenic properties are studies of cancer cells lines that have demonstrated *Slit2* promoter methylation in 59% of the breast, 77% of the non–small cell lung, and 55% of the small cell lung cancer cell lines examined [13]. Epigenetic silencing of *Slit2* has additionally been demonstrated in cases of acute and chronic lymphocytic leukemia [14], glioma [15], renal cell carcinoma [16], cervical cancer [17], and hepatocellular carcinoma [18], in which the level of *Slit2* messenger RNA (mRNA) has also been shown to decrease with increasing metastatic potential [19].

Alternatively, evidence also exists to state that Slit2 possesses an oncogenic function. Avci et al. [20] have reported that Slit2 and Robo1, a Slit2 receptor, can also be upregulated in hepatocellular carcinomas with advanced stages and poor tumor differentiation. In addition, an increase in *Slit2* mRNA has also been noted in canine malignant mammary tumors [21]. Schmid et al. [12] have shown through the use of a transwell migration assay that the addition of Slit2 is capable of inducing direct migration of breast cancer cells and, in an appropriate cell line, may induce brain metastasis. Using a Boyden chamber assay, Wang et al. [22] have demonstrated that Slit2 is capable of attracting endothelial cells. In addition, they have also demonstrated *in vitro* that Slit2 is capable of promoting angiogenic activity, increasing tubular network formation in cancer. Moreover, in a study of pancreatic islet tumors in mice, Yang et al. [23] intercrossed a transgenic mouse overexpressing Slit2 with a nonmetastatic RIP-Tag2 mouse tumor model and noted that the expression of Slit2 enhanced lymphangiogenesis and promoted lymph node metastasis.

To date, only two studies have been conducted to examine the expression of Slit2 in prostate cancer, both of which showed contrasting results. One documented an increase in *Slit2* mRNA expression across multiple cases of prostate cancer, especially those with a hormone refractory status [24]. The other demonstrated promoter hypermethylation of the *Slit2* gene, supporting a hypothesis of reduced gene expression [25].

To our knowledge, the immunoprofiles of Slit2 have not previously been compared between specimens of benign prostate, primary prostate adenocarcinoma, and metastatic prostate adenocarcinoma. Assessing them will provide further information about the expression of Slit2 in prostate cancer, as well as help elucidate its potential as a diagnostic or prognostic biomarker. Here, we compare the immunohistochemical profiles in a series of 11 cases of normal donor prostate (NDP), 35 cases of normal tissue adjacent to prostatic adenocarcinoma (NAC), 15 cases of benign prostatic hyperplasia (BPH), 35 cases of high-grade prostatic intraepithelial neoplasia (HGPIN), 106 cases of primary prostatic adenocarcinoma (PCa), and 37 cases of metastatic prostatic adenocarcinoma (Mets) to examine if either a tumor suppressor or an oncogenic function for Slit2 can be suggested.

Our findings indicate that the overall expression of Slit2 was higher in HGPIN and PCa than in NDP and NAC ($P < .05$), although not all cases of HGPIN and PCa featured high expression levels. Although the overall differences between Mets and the normal tissues were not significant, several Mets cases individually featured high Slit2 staining intensities.

Materials and Methods

Tissue Microarray Block Preparation

Tissue microarray (TMA) blocks were constructed with specimens obtained from the Health Sciences Tissue Bank at the University of Pittsburgh Medical Center. The tissue bank rendered the honest broker services for this study, with all specimens obtained with informed consent. Cores from each specific paraffin-embedded tissue block were assembled into TMAs as previously described [26]. At the selection of the cases for the construction of the initial TMAs, a pathologist selected regions for sampling that maximized the type of tissue defining the core. As such, there are no sections of "normal" tissues that contain cancer. There were very minimal-to-no sections containing normal glandular tissue in the other classifications. The final TMAs consisted of 11 cases of NDP, 35 cases of NAC, 15 cases of BPH, 35 cases of HGPIN, 106 cases of PCa, and 37 cases of Mets. No specimens of HGPIN in this study contained diagnosed PCa. All TMAs were initially prepared so that each case would be represented at least in triplicate. Because of the variations in TMA processing, however, some cases were only able to be represented in duplicate. In such instances, these cases were still included as a part of the final analysis.

Immunohistochemistry

Each TMA block was deparaffinized and then rehydrated with incremental ethanol concentrations. Decloaker was then used for heat induced epitope retrieval, followed by a 5-minute Tris-buffered saline buffer rinse. A Dako autostainer was then used to stain the TMAs with anti-Slit2 (working dilution 1:1600), a rabbit monoclonal antibody (catalog no. 2864-1) from Epitomics (Burlingame, CA). Immunolabeling was conducted using Dako Envision + Rabbit Polymer (catalog no. K4003) from Dako (Carpinteria, CA). The slides were counterstained with hematoxylin and coverslipped.

Scoring of Slides

All slides were scanned as digital whole slides images using ScanScope XT (Aperio, Vista, CA). The individual tissue cores for each whole slide image were viewed using Aperio ImageScope (Version 11.0.2.716) and scored by applying the Positive Pixel Count Algorithm to each one. To detect the Slit2 staining, a hue value of 0.1 and a hue width of 0.5 were chosen for the algorithm, corresponding to the suggested range for the detection of brown immunostaining using the software (*Aperio Positive Pixel Count Algorithm Instruction Manual*). By analyzing the average

pixel intensity with a predetermined hue value and width, the stromal tissue and cell nuclei that appear blue and do not feature the immunostain are negated by the software and excluded from the final analysis that determines the average staining intensity. This, in effect, controls for the glandular to stromal tissue ratio present in the TMA cores. The validity of using Aperio software for quantitative immunohistochemistry has been previously documented [27,28]. The average staining intensity was then determined by the software for each core, using a formula that sums the intensities of weak, moderate, and strong staining pixels and divides this value by the total number of weak, moderate, and strong pixels. Staining intensities for the software are reported on a scale of 0 to 255, corresponding to light transmission through the specimen. Therefore, higher staining intensities correspond to lower scores on the light transmissibility scale. Scores in the range of 220 to 175 are classified as weak staining, 175 to 100 as moderate staining, and 0 to 100 as strong staining. To make staining scores more intuitive in our figures, our results are reported as the difference between no stain detection (255) and the average staining intensity as reported by the software, so that higher values correspond to the higher staining intensities. This value is referred to as the "staining intensity" throughout the rest of the article.

The means for each case and, subsequently, for each tissue type were then determined. For the specimens of adenocarcinoma, the Gleason score and tumor stage, where available, were also reported. The clinical TNM, as opposed to the pathologic TNM, staging classification was used to assess the specimens. All means were reported with SEs.

One-way analysis of variance with subsequent Tukey tests for multiple comparisons ($\alpha = 0.05$) were used to compare the tissue types, PCa carcinoma stages, and PCa Gleason scores. When the assumptions were not met for the parametric analysis, Kruskal-Wallis tests, with subsequent Dunn method for multiple comparisons, were used.

Photomicrographs of tissue cores were obtained using an Olympus BX51 microscope (Olympus, Center Valley, PA) using Spot Advanced V4.6 (Diagnostic Instruments, Inc) software. All images were taken at 20×.

This study received exempt approval (PRO08040368) from the University of Pittsburgh's institutional review board. All authors have read and approved of the final article.

Results

Patients' Ages

Mean ages of patients with SDs for the tissue types in this study were as follows: NDP = 32 ± 13 years, NAC = 64 ± 7 years, BPH = 67 ± 9 years, PIN = 64 ± 8 years, PCa = 65 ± 10 years, and Mets = 70 ± 10 years.

Staining Intensities

Mean staining scores for NDP, BPH, NAC, HGPIN, PCa, and Mets were 113.39 ± 3.38, 123.37 ± 3.74, 116.82 ± 3.05, 142.42 ± 3.63, 135.36 ± 1.91, and 128.7 ± 4.89, respectively (Figure 1). A Kruskal-Wallis test with subsequent Dunn method for multiple comparisons showed significant differences between HGPIN and NDP ($P < .05$), HGPIN and NAC ($P < .05$), PCa and NDP ($P < .05$), and PCa and NAC ($P < .05$).

None (0%) of 11 cases of NDP, 1 (2.9%) of 35 cases of NAC, none (0%) of 15 cases of BPH, 10 (28.6%) of 35 cases of HGPIN, 19 (17.9%) of 106 cases of PCa, and 9 (24.3%) of 37 cases of Mets had average staining scores in the highest intensity category.

When classified by tumor stage, the mean scores were 134.49 ± 3.50 ($n = 39$) in stage II, 133.51 ± 3.02 ($n = 38$) in stage 3, and 138.95 ± 3.37 ($n = 29$) in stage 4 (Figure 2). No significant differences were seen between the stages ($P = .51$).

When classified by Gleason score, the average staining score was 128.25 ± 5.66 ($n = 14$) for those with a score of 6 or less, 135.43 ± 2.76

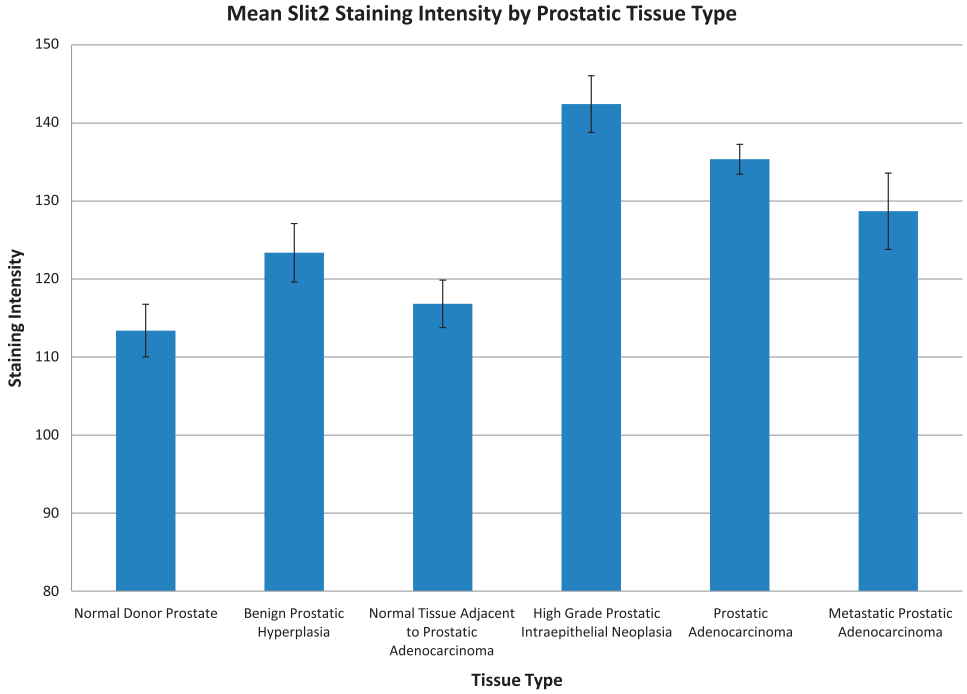

Figure 1. Mean Slit2 staining intensity by prostatic tissue type. Mean Slit2 staining score by prostatic tissue type. Significant differences were seen between HGPIN and NDP ($P < .05$), HGPIN and NAC ($P < .05$), PCa and NDP ($P < .05$), and PCa and NAC ($P < .05$).

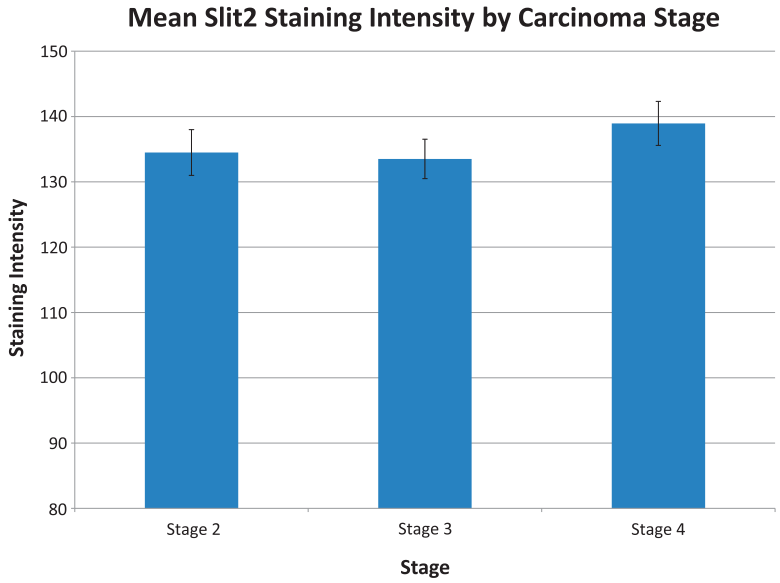

Figure 2. Mean Slit2 staining intensity by carcinoma stage. Mean Slit2 staining intensity by PCa carcinoma stage. No significant differences or trends were observed between the stages ($P = .51$).

($n = 53$) for those with a score of 7, and 137.82 ± 2.95 ($n = 39$) for those with a score of 8 or more (Figure 3). No significant differences were seen between the Gleason score classifications ($P = .30$).

Staining Patterns

Representative photomicrographs of the TMA cores are shown in Figure 4. Across the specimens of all tissue categories, Slit2 featured a diffuse and cytoplasmic staining pattern, with no nuclear or predominant membranous staining pattern noted in the cores. Very minimal-to-no staining for Slit2 was noted in the stromal cells, which were predominantly blue from the hematoxylin counterstaining.

Discussion

In this study, we characterize the immunostaining patterns of Slit2 in primary and metastatic prostate adenocarcinoma. Only one case between the NDP, BPH, and NAC groups featured average staining for Slit2 in the highest intensity category. In contrast, 10 (28.6%) of 35 cases of HGPIN, 19 (17.9%) of 106 cases of PCa, and 9 (24.3%) of 37 cases of Mets had staining scores in the highest intensity category. The overall average staining was highest in the specimens of HGPIN and PCa, with these classifications significantly different than both NDP ($P < .05$) and NAC ($P < .05$) (Figure 1). It is therefore interesting that despite having nine cases of Mets whose staining intensities fell within the highest classification range, the average Mets staining intensity across all cases was not significantly different from the normal tissue groups. This may be explained by the fact that only 11 (10.4%) of 106 cases of PCa had average scores lower than 150, whereas 7 (18.9%) of 37 cases of Mets had average scores lower than 150, which reduced the overall average score for the Mets more that of the PCa group.

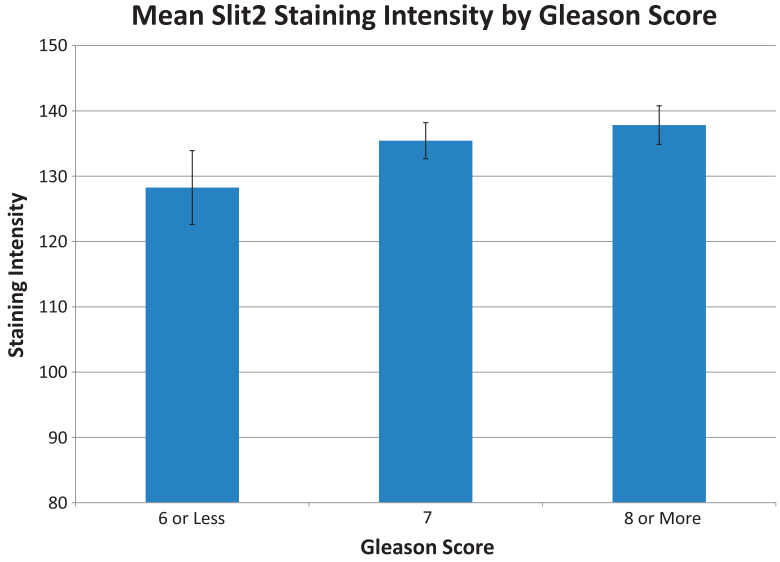

Figure 3. Mean Slit2 staining intensity by Gleason score. Mean Slit2 staining intensity by PCa Gleason score. No significant differences were seen by this classification ($P = .30$), although the staining intensity trended higher with increasing Gleason score.

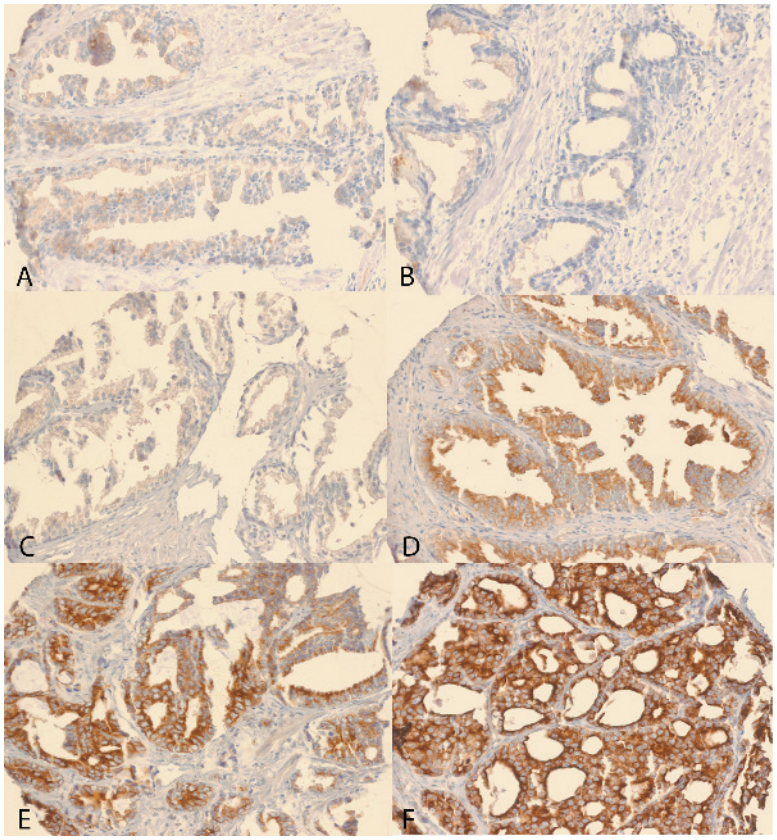

Figure 4. Photomicrographs of TMA cores. Photomicrographs of TMA cores (20×): (A) NDP, (B) BPH, (C) NAC, (D) HGPIN, (E) PCA, and (F) Mets. Note the predominantly cytoplasmic staining pattern, which is higher in intensity in the depicted specimens of HGPIN, PCa, and Mets. Highest category staining was noted in 0 (0%) of 11 cases of NDP, 1 (2.9%) of 35 cases of NAC, 0 (0%) of 15 cases of BPH, 10 (28.6%) of 35 cases of HGPIN, 19 (17.9%) of 106 cases of PCa, and 9 (24.3%) of 37 cases of Mets.

This phenomenon of different staining patterns for Slit2 in prostate cancer has previously been noted by Latil et al. [24], who observed varying levels of *Slit2* mRNA expression across different prostate tumors, with those cancers overexpressing Slit2 typically possessing a hormone-refractory status. Whereas this provides a very plausible mechanism to explain the differences that we observed in this study, information about the hormone-responsive status of these specimens was not available to include in the analysis.

Although our study concurs with that of Latil et al. [24] in showing an increase in the expression of Slit2 in select cases of prostate cancer, Yu et al. [25] have shown that *Slit2* is epigenetically silenced in a majority of metastatic prostate tumors, with the tumorigenic protein EZH2 forming polycomb-repressive complexes capable of binding to the *Slit2* promoter, inhibiting its expression and hence function as a tumor suppressor. Although this may account for its lower levels of expression in several of the metastatic tumors, our data do not indicate that this occurs universally because nine cases of metastatic prostate cancer featured staining scores in the highest categories, whereas only one case of NDP, NAC, or BPH fell within this classification. The cases of metastasis featuring high levels of Slit2 expression in this study included metastasis from the prostate to lymph node, bone, and liver, indicative that more than one metastatic location can be involved in cases of elevated Slit2 expression.

Similarly, differing results for the expression of Slit2 in cancer has been noted across other tissue types. Although promoter hypermethylation, and hence lower gene expression, has been observed in breast cancer tumors and accompanying paired sera [29], other work has demonstrated positive immunostaining for Slit2 in a series of 51 of 72 cases of breast cancer, most commonly in tissue areas with high concentrations of cancer cells [22].

It is also interesting that we did not observe a statistically significant difference in the staining intensities by PCa stage ($P = .51$; Figure 2). Whereas an absolute increase in Slit2 staining was observed with an increasing Gleason score, this difference did not reach statistical significance ($P = .30$; Figure 3). These results stand in contrast to a previous study of hepatocellular carcinoma, where Slit2 expression was found to correlate with advanced stage and poor tumor differentiation [19].

In general, those positing that Slit2 may be linked to tumor suppression have suggested multiple possible physiological mechanisms. In breast cancer, it has been hypothesized that EphA2 receptor tyrosine kinase, an angiogenic regulator that itself has previously been shown to be expressed in tumor vasculature [30,31], represses endothelial Slit2 expression [32]. In a study of Slit2-transfected fibrosarcoma tumor cells, increasing Slit2 expression decreased the expression of the anti-apoptotic molecule Bcl-xl, as well as the cell cycle molecules Cdk6 and Cyclin D1 [33]. Others have suggested that Slit2 signaling decreases activated Cdc42, another cell cycle protein [34,35].

Those proposing an oncogenic role for Slit2 have suggested that it may recruit vascular endothelial cells for angiogenesis within a tumor mass, as recombinant Slit2 protein has been shown to attract endothelial cells and promote tube formation [22]. Others have suggested that

the Slit2 may be increased because of an up-regulation in response to cellular proinflammatory mediators, such as tumor necrosis factor and interleukin 1β, hypoxia, or oncogene expression in cancer [22]. It has also been hypothesized that, in some tumors, Slit2 may stimulate the invasion of tumor cells away from the primary mass [36]. In one study where A375 malignant melanoma cells were pretreated with heparin, increased Slit2 was noted in the supernatant, whereas a decreased concentration was noted in whole cell lysates, which may suggest an interaction between Slit2 and heparin sensitive proteoglycans on cancer cells [22]. In addition, Slit2 has been shown to activate the phosphatidylinositol 3-kinase pathway [22], which has also been previously implicated in oncogenesis [37].

Although, to our knowledge, a definitive reconciliation between these two theories has not been reached, multiple theories for further investigation have been proposed. In cases of metastasis, it has been suggested that a local down-regulation of Slit2 may lead to a metastatic process, whereas receptor sites expressing Slit2 may promote oncogenesis [12]. Others have also observed that a change from a chemoattractant to a chemorepellant response to a Slit protein has been observed in mesodermal tissues [12,38], which also may warrant further investigation. In addition, Song et al. [39] have also shown that the same guidance cues may promote attraction or repulsion in neurons in a manner dependent on cAMP activity, demonstrating that two different functions are possible for a molecular cue depending on its coaccompanying molecular physiology. Because Slit2 is only one molecule in the Slit/Robo signaling pathway, its role in oncogenesis may also be linked to the expression levels of its receptors, as evidenced by the fact that other studies have also linked Robo1 to oncogenesis [20,22,40].

Although all of these possibilities merit further examination, our findings concur with Latil et al. [24] and suggest that a higher expression of Slit2 is more commonly seen in cases of HGPIN, PCa, and Mets than in nonneoplastic tissues. Although, based on our data, Slit2 does not seem to be able to distinguish between PCa and Mets, it still seems to have clinical utility as an important biomarker for prostate cancer.

Conclusions

These results provide a basis for the characterization of the staining patterns and intensities of Slit2 in PCa and Mets in comparison to benign prostate tissues. Slit2 immunostaining was overall significantly higher in specimens of HGPIN and PCa than in benign specimens. Although the overall staining was not higher in Mets compared with benign prostates, several cases of Mets featured high staining intensities for Slit2.

No significant differences or consistent trend was observed when the specimens were compared by stage. Although the staining intensity increased with increasing Gleason score, these differences were also not significant. Slit2 staining was predominantly cytoplasmic in the specimens that we examined across all tissues categories.

Although only one case between the NDP, BPH, and NAC groups featured a staining intensity in the highest category, 10 (28.6%) of 35 specimens of HGPIN, 19 (17.9%) of 106 specimens of PCa, and 9 (24.3%) of 37 specimens of Mets had staining scores in the highest intensity category. Although this study did not indicate that Slit2 can differentiate between specimens of PCa and Mets, it does support previous findings by Latil et al. [24] and suggests that Slit2 may be an important biomarker for prostate cancer.

Acknowledgments

The authors of this article thank Marianne Notaro for assistance with TMA preparation, Marie Acquafondata for assistance with immunohistochemical staining, Michelle Bisceglia for assistance in coordinating tissue bank specimens, and the Clinical Scientist Training Program, funded by the Office of the Dean at the University of Pittsburgh School of Medicine.

References

[1] Jemal A, Siegel R, Xu J, and Ward E (2010). Cancer statistics, 2010. *CA Cancer J Clin* **60**, 277–300.

[2] Etzioni R, Penson DF, Legler JM, di Tommaso D, Boer R, Gann PH, and Feuer EJ (2002). Overdiagnosis due to prostate-specific antigen screening: lessons from U.S. prostate cancer incidence trends. *J Natl Cancer Inst* **94**, 981–990.

[3] Joniau S and Van Poppel H (2008). Localized prostate cancer: can we better define who is at risk of unfavourable outcome? *BJU Int* **101**(suppl 2), 5–10.

[4] Moul JW (2008). Are we overtreating prostate cancer? *J Urol* **180**, 2299–2300.

[5] Chandran UR, Dhir R, Ma C, Michalopoulos G, Becich M, and Gilbertson J (2005). Differences in gene expression in prostate cancer, normal appearing prostate tissue adjacent to cancer and prostate tissue from cancer free organ donors. *BMC Cancer* **5**, 45.

[6] Georgas K, Burridge L, Smith K, Holmes GP, Chenevix-Trench G, Ioannou PA, and Little MH (1999). Assignment of the human slit homologue SLIT2 to human chromosome band 4p15.2. *Cytogenet Cell Genet* **86**, 246–247.

[7] Morlot C, Thielens NM, Ravelli RB, Hemrika W, Romijn RA, Gros P, Cusack S, and McCarthy AA (2007). Structural insights into the Slit-Robo complex. *Proc Natl Acad Sci USA* **104**, 14923–14928.

[8] Wong K, Park HT, Wu JY, and Rao Y (2002). Slit proteins: molecular guidance cues for cells ranging from neurons to leukocytes. *Curr Opin Genet Dev* **12**, 583–591.

[9] Dickson BJ and Gilestro GF (2006). Regulation of commissural axon pathfinding by slit and its Robo receptors. *Annu Rev Cell Dev Biol* **22**, 651–675.

[10] Wu JY, Feng L, Park HT, Havlioglu N, Wen L, Tang H, Bacon KB, Jiang Z, Zhang X, and Rao Y (2001). The neuronal repellent Slit inhibits leukocyte chemotaxis induced by chemotactic factors. *Nature* **410**, 948–952.

[11] Liu D, Hou J, Hu X, Wang X, Xiao Y, Mou Y, and De Leon H (2006). Neuronal chemorepellent Slit2 inhibits vascular smooth muscle cell migration by suppressing small GTPase Rac1 activation. *Circ Res* **98**, 480–489.

[12] Schmid BC, Rezniczek GA, Fabjani G, Yoneda T, Leodolter S, and Zeillinger R (2007). The neuronal guidance cue Slit2 induces targeted migration and may play a role in brain metastasis of breast cancer cells. *Breast Cancer Res Treat* **106**, 333–342.

[13] Dallol A, Da Silva NF, Viacava P, Minna JD, Bieche I, Maher ER, and Latif F (2002). SLIT2, a human homologue of the *Drosophila Slit2* gene, has tumor suppressor activity and is frequently inactivated in lung and breast cancers. *Cancer Res* **62**, 5874–5880.

[14] Dunwell TL, Dickinson RE, Stankovic T, Dallol A, Weston V, Austen B, Catchpoole D, Maher ER, and Latif F (2009). Frequent epigenetic inactivation of the *SLIT2* gene in chronic and acute lymphocytic leukemia. *Epigenetics* **4**, 265–269.

[15] Dallol A, Krex D, Hesson L, Eng C, Maher ER, and Latif F (2003). Frequent epigenetic inactivation of the *SLIT2* gene in gliomas. *Oncogene* **22**, 4611–4616.

[16] Astuti D, Da Silva NF, Dallol A, Gentle D, Martinsson T, Kogner P, Grundy R, Kishida T, Yao M, Latif F, et al. (2004). SLIT2 promoter methylation analysis in neuroblastoma, Wilms' tumour and renal cell carcinoma. *Br J Cancer* **90**, 515–521.

[17] Narayan G, Goparaju C, Arias-Pulido H, Kaufmann AM, Schneider A, Durst M, Mansukhani M, Pothuri B, and Murty VV (2006). Promoter hypermethylation-mediated inactivation of multiple Slit-Robo pathway genes in cervical cancer progression. *Mol Cancer* **5**, 16.

[18] Jin J, You H, Yu B, Deng Y, Tang N, Yao G, Shu H, Yang S, and Qin W (2009). Epigenetic inactivation of SLIT2 in human hepatocellular carcinomas. *Biochem Biophys Res Commun* **379**, 86–91.

[19] Zheng D, Liu BB, Liu YK, Kang XN, Sun L, Guo K, Sun RX, Chen J, and Zhao Y (2009). Analysis of the expression of *Slit/Robo* genes and the methylation status of their promoters in the hepatocellular carcinoma cell lines. *Zhonghua Gan Zang Bing Za Zhi* **17**, 198–202.

[20] Avci ME, Konu O, and Yagci T (2008). Quantification of SLIT-ROBO transcripts in hepatocellular carcinoma reveals two groups of genes with coordinate expression. *BMC Cancer* **8**, 392.

[21] Tanno T, Tanaka Y, Sugiura T, Akiyoshi H, Takenaka S, Kuwamura M, Yamate J, Ohashi F, Kubo K, and Tsuyama S (2006). Expression patterns of the slit subfamily mRNA in canine malignant mammary tumors. *J Vet Med Sci* **68**, 1173–1177.

[22] Wang B, Xiao Y, Ding BB, Zhang N, Yuan X, Gui L, Qian KX, Duan S, Chen Z, Rao Y, et al. (2003). Induction of tumor angiogenesis by Slit-Robo signaling and inhibition of cancer growth by blocking Robo activity. *Cancer Cell* **4**, 19–29.

[23] Yang XM, Han HX, Sui F, Dai YM, Chen M, and Geng JG (2010). Slit-Robo signaling mediates lymphangiogenesis and promotes tumor lymphatic metastasis. *Biochem Biophys Res Commun* **396**, 571–577.

[24] Latil A, Chene L, Cochant-Priollet B, Mangin P, Fournier G, Berthon P, and Cussenot O (2003). Quantification of expression of netrins, slits and their receptors in human prostate tumors. *Int J Cancer* **103**, 306–315.

[25] Yu J, Cao Q, Wu L, Dallol A, Li J, Chen G, Grasso C, Cao X, Lonigro RJ, Varambally S, et al. (2010). The neuronal repellent SLIT2 is a target for repression by EZH2 in prostate cancer. *Oncogene* **29**, 5370–5380.

[26] Kajdacsy-Balla A, Geynisman JM, Macias V, Setty S, Nanaji NM, Berman JJ, Dobbin K, Melamed J, Kong X, Bosland M, et al. (2007). Practical aspects of planning, building, and interpreting tissue microarrays: the Cooperative Prostate Cancer Tissue Resource experience. *J Mol Histol* **38**, 113–121.

[27] Lloyd MC, Allam-Nandyala P, Purohit CN, Burke N, Coppola D, and Bui MM (2010). Using image analysis as a tool for assessment of prognostic and predictive biomarkers for breast cancer: how reliable is it? *J Pathol Inform* **1**, 29.

[28] Bolton KL, Garcia-Closas M, Pfeiffer RM, Duggan MA, Howat WJ, Hewitt SM, Yang XR, Cornelison R, Anzick SL, Meltzer P, et al. (2010). Assessment of automated image analysis of breast cancer tissue microarrays for epidemiologic studies. *Cancer Epidemiol Biomarkers Prev* **19**, 992–999.

[29] Sharma G, Mirza S, Prasad CP, Srivastava A, Gupta SD, and Ralhan R (2007). Promoter hypermethylation of $p16^{INK4A}$, p14ARF, CyclinD2 and Slit2 in serum and tumor DNA from breast cancer patients. *Life Sci* **80**, 1873–1881.

[30] Brantley-Sieders DM and Chen J (2004). Eph receptor tyrosine kinases in angiogenesis: from development to disease. *Angiogenesis* **7**, 17–28.

[31] Pasquale EB (2010). Eph receptors and ephrins in cancer: bidirectional signalling and beyond. *Nat Rev Cancer* **10**, 165–180.

[32] Brantley-Sieders DM, Dunaway CM, Rao M, Short S, Hwang Y, Gao Y, Li D, Jiang A, Shyr Y, Wu JY, et al. (2011). Angiocrine factors modulate tumor proliferation and motility through EphA2 repression of Slit2 tumor suppressor function in endothelium. *Cancer Res* **71**, 976–987.

[33] Kim HK, Zhang H, Li H, Wu TT, Swisher S, He D, Wu L, Xu J, Elmets CA, Athar M, et al. (2008). Slit2 inhibits growth and metastasis of fibrosarcoma and squamous cell carcinoma. *Neoplasia* **10**, 1411–1420.

[34] Xu Y, Li WL, Fu L, Gu F, and Ma YJ (2010). Slit2/Robo1 signaling in glioma migration and invasion. *Neurosci Bull* **26**, 474–478.

[35] Werbowetski-Ogilvie TE, Seyed Sadr M, Jabado N, Angers-Loustau A, Agar NY, Wu J, Bjerkvig R, Antel JP, Faury D, Rao Y, et al. (2006). Inhibition of medulloblastoma cell invasion by Slit. *Oncogene* **25**, 5103–5112.

[36] Mertsch S, Schmitz N, Jeibmann A, Geng JG, Paulus W, and Senner V (2008). Slit2 involvement in glioma cell migration is mediated by Robo1 receptor. *J Neurooncol* **87**, 1–7.

[37] Carnero A, Blanco-Aparicio C, Renner O, Link W, and Leal JF (2008). The PTEN/PI3K/AKT signalling pathway in cancer, therapeutic implications. *Curr Cancer Drug Targets* **8**, 187–198.

[38] Kramer SG, Kidd T, Simpson JH, and Goodman CS (2001). Switching repulsion to attraction: changing responses to slit during transition in mesoderm migration. *Science* **292**, 737–740.

[39] Song HJ, Ming GL, and Poo MM (1997). cAMP-induced switching in turning direction of nerve growth cones. *Nature* **388**, 275–279.

[40] Grone J, Doebler O, Loddenkemper C, Hotz B, Buhr HJ, and Bhargava S (2006). Robo1/Robo4: differential expression of angiogenic markers in colorectal cancer. *Oncol Rep* **15**, 1437–1443.